DOI: 10.1002/ejic.200500593

Intense Near-Infrared Luminescence of a Mesomorphic Ionic Liquid Doped with Lanthanide β-Diketonate Ternary Complexes

Lada N. Puntus,[a,c] Kurt J. Schenk,[b] and Jean-Claude G. Bünzli*[c]

Keywords: Ionic liquids / Liquid crystals / Lanthanides / Near infrared luminescence / Quantum yield / Small-angle X-ray diffraction

The ionic liquid 1-dodecyl-3-methylimidazole chloride ([C_{12}-mim]Cl) is doped with 1 mol-% of the lanthanide ternary complexes [Ln(tta)$_3$(phen)] (tta = thenoyltrifluoroacetonate, phen = 1,10-phenanthroline, Ln = Nd, Eu, Er, Yb), resulting in luminescent mesogenic phases at room temperature. According to DSC and SAXS measurements, the temperature of the crystal → liquid crystal transition is below 10 °C. Analysis of vibrational and luminescence data points to the inner co-ordination sphere of the Eu^{III} ion being very similar in both the mesomorphic sample and the parent β-diketonate complex. The mesomorphic samples containing Nd^{III}, Er^{III}, or Yb^{III} display relatively intense near-infrared luminescence. This emission is enhanced in the liquid crystalline phases with respect to the initial compounds, as demonstrated for instance by the quantum yield of the [Yb(tta)$_3$(phen)]-containing mesogenic sample which amounts to 2.1 %, as compared to 1.6 and 1.1 % for the powdered ternary complex and its solution in toluene, respectively.

Introduction

The development of smaller, more penetrable probes for biological imaging using near-infrared (NIR) light,[1,2] as well as of luminescent polymers for optical amplifiers[3] and light-emitting diodes working in the telecommunication window (1–1.6 μm)[4] have attracted a lot of attention recently. In this context, near-infrared lanthanide-based emitters are presenting considerable interest in view of their peculiar spectroscopic properties, namely narrow and easily recognizable emission lines and relatively long lifetimes of their excited states, compared with organic chromophores, which allows the use of time-resolved spectroscopy in analytical procedures, thus enhancing considerably the signal-to-noise ratio. In recent papers, we have demonstrated how Yb($^2F_{5/2}$) can be populated through energy transfer from Cr^{III} in a heterobimetallic d-f helicate, leading to an apparent lengthening of the Yb^{III} lifetime in the ms range,[5,6] and we have proposed an octadentate podand yielding highly stable and luminescent complexes in water.[7]

Liquid crystalline phases provide anisotropic media which are used in displays (LCD) and succeeding in producing emissive LCD by rendering the liquid crystalline phase luminescent would be a definitive advantage.[8] In addition, NIR-emitting mesomorphic materials could be useful in optical telecommunications since they would act as switchable light-converting devices. One strategy for producing lanthanide-containing mesophases is the doping of existing liquid crystalline phases with luminescent lanthanide salts and complexes.[9–16] For instance, we have recently shown how the emission color of a room temperature ionic liquid (RTIL) presenting a liquid crystalline phase at room temperature, 1-dodecyl-3-methylimidazolium chloride ([C_{12}-mim]Cl) can be tuned by the introduction of various Eu^{III} salts and by varying the excitation wavelength.[10] Ionic liquids present definitive advantages over classical solvents,[17–19] and some of them have been used for generating lanthanide-containing solutions emitting in the NIR range.[20,21] In this paper, we report the thermal, structural, and photophysical properties of solutions of lanthanide tris(thenoyltrifluoroacetylacetonate)[22] with *o*-phenanthroline in [C_{12}-mim]Cl and demonstrate an exaltation of their NIR-emitting properties with respect to solutions of these complexes in toluene and in the solid state.

Results and Discussion

Characterization of the Mesophases

Imidazolium chlorides with long alkyl chains form lamellar arrays in the crystalline phase and an enantiomeric

[a] Russian Academy of Sciences, Institute of Radio-Engineering and Electronics,
125009 Moscow, Russia
E-mail: lada_puntus@mail.ru
[b] Laboratory of Crystallography, École Polytechnique Fédérale de Lausanne, BSP,
1015 Lausanne, Switzerland
E-mail: kurt.schenk@epfl.ch
[c] Laboratory of Lanthanide Supramolecular Chemistry, École Polytechnique Fédérale de Lausanne, BCH 1405,
1015 Lausanne, Switzerland
E-mail: jean-claude.bunzli@epfl.ch
Supporting information for this article is available on the WWW under http://www.eurjic.org or from the author.

smectic liquid crystalline phase (SmA_2) at higher temperature.[23] The temperature of the crystal→smectic A_2 transition of [C_{12}-mim]Cl heavily depends on hydration (44.5 °C for the monohydrate and –2.8 °C for an anhydrous salt) owing to the significant structural stabilization induced by hydrogen bonds with water molecules. The H-bond array is destroyed at elevated temperature and under vacuum, which allowed Guillet et al.[10] to obtain 10 mol-% solutions of Eu salts (chloride, nitrate, perchlorate, and triflate) in [C_{12}-mim]Cl without disturbing the mesomorphic properties of this RTIL. In our case, the [Ln(tta)$_3$(phen)] complexes are too sensitive to thermal decomposition and since they have low solubility in anhydrous [C_{12}-mim]Cl, we have settled for a partially dehydrated ionic liquid (<1 water molecule per molecule of ionic liquid, probably around 0.25), in which 1 mol-% solutions of ternary complexes could be prepared. In the following description, we use **Ln1** to designate the samples prepared in this way. DSC data indicate the formation of a SmA_2 phase starting between 6 and 10 °C and ending by isotropization between 99 and 102 °C for all the Ln-containing materials obtained (Figure 1).

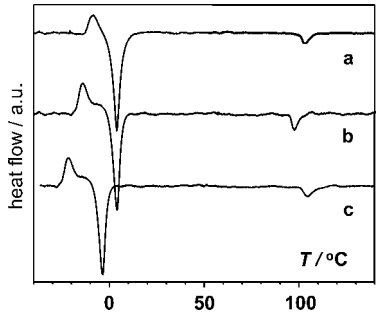

Figure 1. DSC traces (first heating-cooling cycle) of (a) **Nd1**, (b) partially dehydrated [C_{12}-mim]Cl and (c) anhydrous [C_{12}-mim]Cl.

We have resorted to small-angle X-ray scattering (SAXS) experiments to get more insight into a correlation between the structural and liquid crystalline properties of the doped mesophases. Data were collected both for the monohydrated imidazolium salt and the **Eu1** sample as a function of temperature and typical SAXS patterns are shown on Figure 2. At room temperature the most intense peak in the low-angle region (2θ = 1.89°) is assigned to the (001) layer repeat unit in the [C_{12}-mim]Cl·H_2O structure with d spacing of 46.6 Å (Figure 2c, Table 1). This d value corresponds to the double/extended bilayer spacing and is reported for the first time for [C_{12}-mim]Cl·H_2O. Similar values of layer spacing have been determined for [C_n-mim]Cl·H_2O with longer alkyl chains (n = 14, 16, 18).[23] Another, less intense peak at 2θ = 3.80° corresponds to a layer spacing of 23.3 Å and is assigned to the (002) regular repeat unit. In addition, a very weak peak at 2θ = 2.79° reveals the presence of a small amount of anhydrous [C_{12}-mim]Cl under its liquid crystalline SmA_2 phase (d = 31.8 Å). At 90 °C only one intense peak is observed at 2θ = 3.08°, corresponding to a layer spacing of 28.7 Å, and is characteristic of the SmA_2 phase. The latter value of the d spacing, as well as the one found for the crystalline phase (d = 23.3 Å) are slightly different from the ones reported by Bradley et al. for fully anhydrous [C_{12}-mim]Cl (22.5 Å in the crystalline phase and 31.7 Å in the SmA_2 phase determined on cooling the isotropic phase[23]). On the other hand, Guillet et al. have extracted a d value of 22.8 Å from the crystal structure of [C_{12}-mim]-Cl·H_2O.[10] These small differences may originate from the hydration state and thermal history of the sample (whether partial or full dehydration was performed) and from the SAXS experimental conditions (during heating or cooling cycles and from which phase SAXS data were collected).[23,24] Depending on these factors different phases such as the extended bilayer and/or double bilayer structures can form both in the initial crystalline phase and in the subsequent re-crystallization process after isotropization. The SAXS pattern for **Eu1** prepared from the previously partially dehydrated imidazolium salt, which feature a single peak at 2θ = 2.79° (Figure 2, a), is totally consistent with the presence of the SmA_2 phase at 26 °C (d = 31.8 Å) similar to that found for pure [C_{12}-mim]Cl (Figure 2, b). Thus, both DSC and SAXS data point to **Ln1** having a structural behavior close to the one of anhydrous [C_{12}-mim]-Cl and therefore, the experimental procedure proposed for preparing the **Ln1** samples successfully produces Ln-containing phases with mesomorphic SmA_2 properties at room temperature.

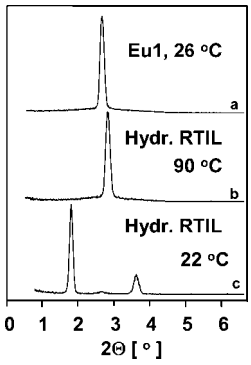

Figure 2. SAXS patterns for **Eu1** at 26 °C (a) and for [C_{12}-mim]-Cl·H_2O at 90 °C (b) and 22 °C (c) obtained during the heating.

Table 1. Layer spacing determined for the crystalline and SmA_2 phases from the position of the lowest-angle diffraction peak.

Sample	T [°C]	Layer spacing (d) [Å]	Phase[a]
[C_{12}-mim]Cl·H_2O	22	23.3 (46.6[b])	Cr
	90	28.7	LC
Eu1	26	31.8	SmA_2

[a] Cr = crystalline, LC = liquid crystalline. [b] Peak due to double/extended bilayer spacing.

Photophysical Properties

The Eu-containing samples have been used to probe changes in the local structure of the lanthanide ions upon the transition from both the crystalline to the liquid crystalline phase and from the solid state to the solution. The crys-

tal-field splitting of the $^5D_0$–^7F_J transitions (J = 1–4), which is very sensitive to differences in the nearest environment of Eu^{III} are alike for all samples, except for some broadening which masks finer details in the luminescence spectra of **Eu1** and of [Eu(tta)$_3$(phen)] in toluene (Figure 3). In the luminescence spectra of powdered [Eu(tta)$_3$(phen)] and **Eu1**, emission from the $^5D_1$ level is also detected, pointing to a not so fast nonradiative relaxation from $^5D_1$ to $^5D_0$ (Figure 4). The luminescence spectra of all the Eu^{III}-containing compounds reveal maximum (2J +1) splitting of the ^7F_J electronic levels, consistent with a low symmetry (at most C_{2v}) of the immediate Eu^{III} surroundings. Judging from the qualitative criterion of the integrated intensity of the $^5D_0 \rightarrow {}^7F_0$ transition relative to the magnetic dipole $^5D_0 \rightarrow {}^7F_1$ transition, the symmetry around the metal ion seems to be lower in the mesophase compared to the powdered sample (0.14 and 0.17, respectively).

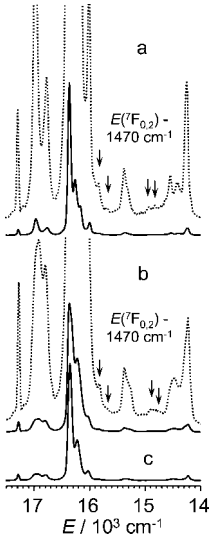

Figure 3. Luminescence spectra at 295 K of (a) [Eu(tta)$_3$(phen)] (solid state), (b) **Eu1**, and (c) [Eu(tta)$_3$(phen)] 10^{-3} M in toluene with inserts showing the vibronic satellites associated to $^5D_0 \rightarrow {}^7F_0$ and $^5D_0 \rightarrow {}^7F_2$ transitions; the excitation wavelength is 385 nm.

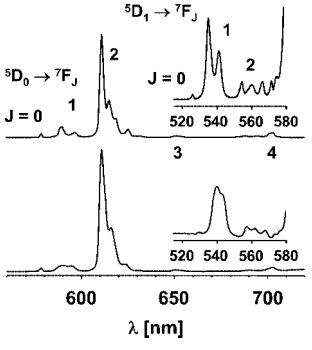

Figure 4. Luminescence spectra of [Eu(tta)$_3$(phen)] (top) and **Eu1** (bottom) at 295 K obtained under ligand excitation at 385 nm.

Both broad structured bands of the ligands and narrow lines of f-f transitions are observed in all the excitation spectra of **Ln1** (Figure 5). These spectra are similar and their coincidence with the absorption spectra indicates a sizeable energy transfer from the ligands onto the lanthanide ion. A broad shoulder with a low-frequency edge at 19665 cm^{-1} and a maximum around 22200 cm^{-1} is most remarkable in the spectrum of [Eu(tta)$_3$(phen)]. Its absence in the excitation spectrum of **Nd1** allows one to assign it to a ligand→metal charge transfer (LMCT) transition. The mean optical electronegativity[25] is equal to χ_{opt} = 2.73, a value obtained by using the optical electronegativity of Eu^{III} reported by Demirbilek et al.[26] This value can then be used to estimate the energy of the LMCT states in the complexes with the other lanthanide ions (Table 2). According to these calculated energies, influence of the LMCT state on the energy migration within the ternary complex should be much smaller in the cases of NIR-emitting ions compared to Eu^{III}.

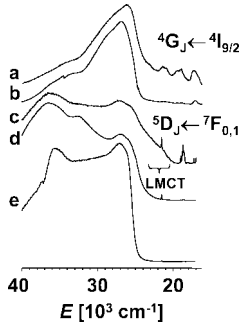

Figure 5. Luminescence excitation spectra of (a) [Nd(tta)$_3$(phen)] (solid state), (b) **Nd1**, (c) [Eu(tta)$_3$(phen)] (solid state), (d) **Eu1**, and (e) [Eu(tta)$_3$(phen)] 10^{-3} M in toluene; λ_{an} are 614 (Eu) and 1060 nm (Nd).

Table 2. Lifetimes of the Ln excited state at room temperature and energy of $^1\pi\pi^*$, $^3\pi\pi^*$, and LMCT states for powdered [Ln(tta)$_3$(phen)] and **Ln1** samples.

Compound	τ_{obs} [μs]	$E(^1\pi\pi^*)$ [cm^{-1}][a]	$E(^3\pi\pi^*)$ [cm^{-1}][b]	E(LMCT) [cm^{-1}][c]
[Nd(tta)$_3$(phen)]	1.29 ± 0.03	24690	20400	40200
Nd1	1.52 ± 0.01	24845		–
[Er(tta)$_3$(phen)]	1.86 ± 0.02	24855	20480	44400
Er1	1.95 ± 0.04	24940		–
[Yb(tta)$_3$(phen)]	12.01 ± 0.02	23920	20340	27900
Yb1	12.4 ± 0.03	24235		–

[a] From fluorescence spectra at 295 K. [b] From phosphorescence spectra at 77 K. [c] Calculated values, see text.

To help characterize the liquid crystalline phases, we have resorted to vibronic satellites appearing in the emission spectra of the Eu-containing samples. They are similar for powdered and mesomorphic samples and the most intense ones are assigned to the symmetric vibration of the β-diketonate chelating ring with a large contribution of the C···O bond stretching with a frequency of 1470 cm^{-1} (Figure 3, cf. the bands marked by arrows in the 15900–15600 and 15110–14800 cm^{-1} spectral ranges). A comparison with the IR spectra of [C_{12}-mim]Cl·H_2O, [Yb(tta)$_3$(phen)], and **Yb1** reveals a homogeneous mixture of both components in the doped liquid crystalline sample (Figure S1, Supporting Information): vibrations of both the ionic liquid and the β-

diketonate complex (although very weak) are indeed seen in the IR spectrum.

On the other hand, the lifetime of the Eu($^5D_0$) state hints at some differences between **Eu1** and the powdered sample. Both luminescence decays are single exponential, but lifetimes amount to 0.64 ± 0.02 and 0.97 ± 0.03 ms for **Eu1** and [Eu(tta)$_3$(phen)], respectively. The shorter lifetime in the former could be explained as follows. In a fluent system, energy transfer quenching involves collisions between complexes during diffusion.[27] The critical distance for nonradiative energy transfer, as calculated from known theory for energy transfer via electric dipole-dipole interaction[28,29] is larger than the collision distance, which leads to energy transfer via cross-relaxation and excitation migration. Moreover, collisional deactivation with [C_{12}-mim]$^+$ cations should also be taken into account. In summary, the luminescence analysis of **Eu1** confirms that dissolution of [Eu(tta)$_3$(phen)] in the RTIL does not modify substantially the inner co-ordination sphere of the europium ion, although it reveals an influence of the ionic liquid on the deactivation processes.

NIR Luminescence

The luminescence excitation spectra of NIR-emitting lanthanide complexes as well as the corresponding **Ln1** (Ln = Nd, Er, Yb) samples are similar (Figure S2, Supporting Information). Comparison of the normalized excitation spectra of powdered and mesophase samples reveals a much lower excitation efficiency of the lanthanide ions through ligand levels in the powdered samples. This reduced luminescence efficiency at high concentration is known as concentration quenching. In spite of the low concentration of the doped ternary complex (1 mol-%), relatively intense luminescence is obtained for all the **Ln1** samples, as ascertained by the intensity ratios found between the total integrated emission intensity of the pure complexes and that of the **Ln1** samples: 6, 3, and 5 for Nd, Er, and Yb, respectively. The near-infrared luminescence spectra of mesomorphic **Ln1** samples at room temperature are presented in Figure 6 and relevant photophysical data are given in Table 2. The observed f-f emission bands correspond to the typical electronic transitions of the NIR-emitting lanthanide ions: $^4F_{3/2}\rightarrow{}^4I_J$ (J = 9/2, 11/2, 13/2) for Nd, $^4I_{13/2}\rightarrow{}^4I_{15/2}$ for Er, and $^2F_{5/2}\rightarrow{}^2F_{7/2}$ for Yb. We have determined the quantum yields of the Yb-centered luminescence taking [Yb(tta)$_3$(H$_2$O)$_2$] as standard. Upon excitation at 390 nm, the quantum yield of **Yb1** amounts to 2.1 ± 0.3%, compared with 1.1 ± 0.1% for a solution of [Yb(tta)$_3$(phen)] in toluene and 1.6 ± 0.2% for a solid-state sample of [Yb(tta)$_3$(phen)] (Figure 6). Thus, the quantum efficiency increases in the order **Yb1** > [Yb(tta)$_3$(phen)] powdered > [Yb(tta)$_3$(phen)] solution, which agrees well with the corresponding lengthening of the emission lifetime. This correlation means that nonradiative relaxation processes are minimized in the ionic liquid used. The improvement in the photophysical properties of the **Ln1** samples is further substantiated by the lifetimes of the metal-centered excited states, which are slightly longer compared with those of the pure ternary complexes (Table 2).

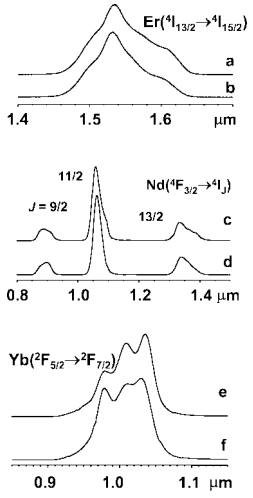

Figure 6. Near-infrared photoluminescence of (a) [Er(tta)$_3$(phen)], (b) **Er1**, (c) [Nd(tta)$_3$(phen)], (d) **Nd1**, (e) [Yb(tta)$_3$(phen)], and (f) **Yb1** at 295 K. The excitation wavelength is 385 nm.

At room temperature, [C_{12}-mim]Cl displays a bright-blue fluorescence with a maximum at 410 nm upon excitation between 225 and 280 nm.[10] Therefore, both a sensitization of the lanthanide-centered NIR luminescence and fluorescence from the RTIL are obtained upon UV excitation. Moreover, owing to the energy transfer from the ionic liquid, lanthanide-centered luminescence can be observed with excitation wavelengths as large as 410 nm (cf. Figures 5, 7, and S2), which is interesting because getting near-infrared emission upon excitation by visible light is an attractive aim for various industrial and analytical applications.

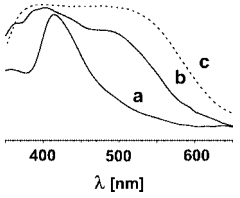

Figure 7. Luminescence spectra of (a) [Nd(tta)$_3$Phen] (solid state), (b) **Nd1** and (c) [C_{12}-mim]Cl at 295 K. The excitation wavelength is 385 nm.

Conclusions

In summary, a method for obtaining [C_{12}-mim]Cl mesophases doped by 1 mol-% [Ln(tta)$_3$(phen)] complexes at room temperature has been developed. The layer spacing in the liquid crystalline phases is independent of the presence of 1 mol-% of [Ln(tta)$_3$(phen)] complexes and identical with the one measured for the anhydrous ionic liquid.[23] The prepared **Ln1** samples have an enantiomeric smectic liquid crystalline phase in the temperature range 10–102 °C. The inner co-ordination sphere of the lanthanide ion remains

essentially unchanged, while the photoluminescence properties are enhanced. The studied liquid crystalline phases display relatively intense near-infrared photoluminescence, thus opening up interesting perspectives for the design of NIR-emitting materials since emission lines from 0.9 to 1.6 μm are easily obtained at the expense of a small amount of β-diketonate complexes (1 mol-%) and since sensitization of this luminescence can be obtained with visible light.

Experimental Section

All reagents and solvents were used as received (Acros); monohydrate of 1-dodecyl-3-methylimidazolium chloride ([C_{12}-mim]Cl·H_2O, Scheme 1)[23] as well as the lanthanide ternary complexes [Ln(tta)$_3$(phen)][30] where Ln = Nd, Eu, Er, Yb were synthesized according to literature procedures and characterized by elemental analyses, IR, and NMR spectroscopy. Thermogravimetric analyses (TGA) under normal atmospheric pressure showed the monohydrated imidazolium salt losing one water molecule per formula weight between 120 and 150 °C and no degradation occurring until 320 °C but decomposition started at 330 °C. In order to obtain a mesophase material at room temperature and to avoid thermal decomposition, the ionic liquid was dehydrated before the introduction of the lanthanide compounds, although complete dehydration was avoided because [Ln(tta)$_3$(phen)] complexes have very low solubility in anhydrous [C_{12}-mim]Cl. All preparations were performed under N_2 using Schlenk techniques and further handling of the samples was performed in a glove-box. Monohydrated [C_{12}-mim]Cl·H_2O was heated from room temperature to 230 °C at a speed of 10 °C/min and under reduced pressure (6.5×10^{-1} Torr), left 5 min at this temperature and then cooled to room temp. The resulting partially dehydrated RTIL showed a crystal → liquid crystal (Cr-LC) transition at 6 °C and isotropization (LC-I transition) at 99 °C. Determination of the transition temperature was performed by means of differential scanning calorimetry (DSC) experiments during the first heating from –90 to 160 °C (Table 3). A DSC experiment was carried out every time before addition of the lanthanide ternary complex for confirmation of the partial dehydration of ionic liquid. Then the lanthanide complexes (1 mol-%) were added to the molten ionic liquid and the mixtures were stirred for 30 min at 130 °C under vacuum. The thermal properties of the Ln-containing samples were tested by DSC again and temperatures of the phase transitions for prepared samples are reported in Table 1. The following notation is used for the samples: **Nd1**, **Eu1**, **Er1**, **Yb1**. Heating the mixtures at higher temperature and during a longer span of time allows the doping of larger quantities of ternary complexes in [C_{12}-mim]Cl but we observed some thermal decomposition. The mesomorphic samples were transferred into 0.1-cm quartz Suprasil® cells under controlled atmosphere and the cells were sealed with paraffin.

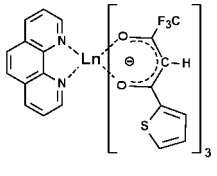

[Ln(tta)$_3$(phen)]

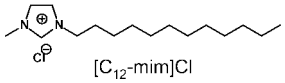

[C_{12}-mim]Cl

Scheme 1.

Table 3. Transition temperatures (in °C, ± 0.5 °C) of the studied samples prepared from partially de-hydrated [C_{12}-mim]Cl (see text), as determined from DSC curves during the first heating-cooling cycle.

Sample	Cr-LC	LC-I	I-LC	LC-Cr
[C_{12}-mim]Cl[a]	6	99	89	3
Nd1	6	102	90	3
Eu1	10	102	93	5
Er1	6	102	89	4
Yb1	9	99	89	2

[a] Partially dehydrated.

Elemental analyses were performed by the Ilse Beetz Laboratory (96301 Kronach, Germany). IR spectra were obtained with a Perkin–Elmer Spectrum One FT-IR spectrometer equipped with a Universal ATR sampling accessory. DSC thermograms were recorded with a Setaram DSC 131 instrument equipped with a liquid nitrogen cooler under nitrogen with cooling-heating cycles between –90 and 160 °C at a rate of 10 °C/min. Thermogravimetric traces were obtained with a Pyris 6 thermogravimetric analyzer from Perkin–Elmer. UV/Visible spectra were measured at 295 K with a Perkin–Elmer Lambda 900 spectrometer. Luminescence measurements (spectra and lifetimes) were recorded with a Fluorolog FL3-22 spectrometer from Jobin–Yvon at 295 and 77 K. Lifetimes for NIR-emitting lanthanides were determined with a high resolution instrumental set-up equipped with a Hamamatsu H9170-75 photomultiplier as described previously.[5] The quantum yields of **Yb1** and of the solution of [Yb(tta)$_3$(phen)] in toluene were determined upon ligand excitation and taking [Yb(tta)$_3$-(H_2O)$_2$] as standard (0.35% in toluene at room temp.).[31] Refractive indices were 1.4964 for the toluene solutions and 1.5059 for **Yb1**.[10] The quantum yield of a powdered sample of [Yb(tta)$_3$-(phen)] was measured by means of an integration sphere from Spex-Jobin Yvon-Horiba 99FL-PLQY, using a described procedure.[32] SAXS patterns were recorded, on samples in 1-mm borosilicate capillaries from Hilgenberg sealed with Araldite®, with a SAXS system from Molecular Metrology equipped with a Cu-K_α Bede micro source configured with confocal Max-Flux™ optics, a variable-temperature universal sample chamber, and a two-dimensional multi-wire gas detector; analysis was performed with the open-source analysis software from Molecular Metrology. The diffraction patterns of pure [C_{12}-mim]Cl were isotropic, whereas those for **Eu1** were somewhat anisotropic. The traces reported in Figure 2 are azimuthally averaged. The Electronic Supporting Information contains IR spectra and excitation luminescence spectra of pure and doped ionic liquids.

Acknowledgments

This work is supported by the Swiss National Science Foundation (National Research Program 47). We thank F. Gumy and D. Baumann for their help in measuring the luminescence lifetimes and obtaining thermal data as well as Frédéric Thomas for the synthesis of [C_{12}-mim]Cl·H_2O.

[1] R. Weissleder, V. Ntziachristos, *Nature Med.* **2003**, *9*, 123–128.
[2] S. Faulkner, S. J. A. Pope, B. P. Burton-Pye, *Appl. Spectrosc. Rev.* **2005**, *40*, 1–31.
[3] G. A. Hebbink, J. W. Stouwdam, D. N. Reinhoudt, F. C. J. M. Van Veggel, *Adv. Mater.* **2002**, *14*, 1147–1150.

[4] T. S. Kang, B. S. Harrison, M. Bouguettaya, T. J. Foley, J. M. Boncella, K. S. Schanze, J. R. Reynolds, *Adv. Funct. Mater.* **2003**, *13*, 205–210.
[5] S. Torelli, D. Imbert, M. Cantuel, G. Bernardinelli, S. Delahaye, A. Hauser, J.-C. G. Bünzli, C. Piguet, *Chem. Eur. J.* **2005**, *11*, 3228–3242.
[6] D. Imbert, M. Cantuel, J.-C. G. Bünzli, G. Bernardinelli, C. Piguet, *J. Am. Chem. Soc.* **2003**, *125*, 15698–15699.
[7] D. Imbert, S. Comby, A.-S. Chauvin, J.-C. G. Bünzli, *Chem. Commun.* **2005**, 1432–1434.
[8] K. Binnemans, C. Görller-Walrand, *Chem. Rev.* **2002**, *102*, 2303–2345.
[9] K. Driesen, K. Binnemans, *Liq. Cryst.* **2004**, *31*, 601–605.
[10] E. Guillet, D. Imbert, R. Scopelliti, J.-C. G. Bünzli, *Chem. Mater.* **2004**, *16*, 4063–4070.
[11] R. Van Deun, D. Moors, B. De Fre, K. Binnemans, *J. Mater. Chem.* **2003**, *13*, 1520–1522.
[12] K. Binnemans, D. Moors, *J. Mater. Chem.* **2002**, *12*, 3374–3376.
[13] J. Boyaval, C. Li, F. Hapiot, M. Warenghem, N. Isaert, Y. Guyot, G. Boulon, P. Carette, *Mol. Cryst. Liq. Cryst.* **2001**, *359*, 337–350.
[14] K. Binnemans, C. Bex, R. Van Deun, *J. Incl. Phenom. Mol. Recogn. Chem.* **1999**, *35*, 63–73.
[15] J. Boyaval, F. Hapiot, C. Li, N. Isaert, M. Warenghem, P. Carette, *Mol. Cryst. Liq. Cryst.* **1999**, *330*, 1387–1394.
[16] L. J. Yu, M. M. Labes, *Appl. Phys. Lett.* **1977**, *31*, 719–720.
[17] P. Wasserscheid, T. Welton, *Ionic Liquids in Synthesis*, Wiley-VCH, Weinheim, **2005**.
[18] G. Moutiers, I. Billard, *Techniques de l'Ingénieur* **2004**, Report AF 6 712.
[19] T. Welton, *Chem. Rev.* **1999**, *99*, 2071–2083.
[20] S. Arenz, A. Babai, K. Binnemans, K. Driesen, R. Giernoth, A.-V. Mudring, P. Nockemann, *Chem. Phys. Lett.* **2005**, *402*, 75–79.
[21] K. Driesen, P. Nockemann, K. Binnemans, *Chem. Phys. Lett.* **2004**, *395*, 306–310.
[22] K. Binnemans in *Handbook on the Physics and Chemistry of Rare Earths* (Eds.: K. A. Gschneidner Jr., J.-C. G. Bünzli, V. K. Pecharsky), Elsevier, Amsterdam, **2005**, vol. 35, ch. 225.
[23] A. E. Bradley, C. Hardacre, J. D. Holbrey, S. Johnston, S. E. J. McMath, M. S. Nieuwenhuizen, *Chem. Mater.* **2002**, *14*, 629–635.
[24] A. Downard, M. J. Earle, C. Hardacre, S. E. J. McMath, M. Nieuwenhuyzen, S. J. Teat, *Chem. Mater.* **2004**, *16*, 43–48.
[25] C. K. Jörgensen, *Mol. Phys.* **1962**, *5*, 271–277.
[26] R. Demirbilek, J. Heber, S. I. Nikitin, *Proceedings of SPIE* **2002**, *4766*, 47–50.
[27] Y. Hasegawa, Y. Wada, S. Yanagida, *J. Photochem. Photobiol. C: Photochem. Rev.* **2004**, *5*, 183–202.
[28] T. Förster, *Ann. Phys.* **1948**, *2*, 55–75.
[29] D. L. Dexter, *J. Chem. Phys.* **1953**, *21*, 836–850.
[30] L. R. Melby, N. J. Rose, E. Abramson, J. C. Caris, *J. Am. Chem. Soc.* **1964**, *86*, 5117–5117.
[31] S. B. Meshkova, Z. M. Topilova, D. V. Bolshoy, S. V. Beltyukova, M. P. Tsvirko, V. Y. Venchikov, *Acta Phys. Pol. A* **1999**, *95*, 983–990.
[32] S. Wrighton, D. S. Ginley, D. L. Morse, *J. Phys. Chem.* **1974**, *78*, 2229–2233.

Received: July 5, 2005
Published Online: October 25, 2005

